



Published in final edited form as:

Eur J Mass Spectrom (Chichester). 2018 February ; 24(1): 157–167. doi:10.1177/1469066717731900.

Structural elucidation of fucosylated chondroitin sulfates from sea cucumber using FTICR-MS/MS

Isaac Agyekum¹, Lauren Pepi¹, Yanlei Yu², Junhui Li³, Lufeng Yan³, Robert J Linhardt², Shiguo Chen³, and I Jonathan Amster¹

¹Department of Chemistry, University of Georgia, Athens, USA

²Department of Chemistry and Chemical Biology, Center for Biotechnology and Interdisciplinary Studies, Rensselaer Polytechnic Institute, Troy, USA

³Department of Food Science and Nutrition, Zhejiang University, China

Abstract

Fucosylated chondroitin sulfates are complex polysaccharides extracted from sea cucumber. They have been extensively studied for their anticoagulant properties and have been implicated in other biological activities. While nuclear magnetic resonance spectroscopy has been used to extensively characterize fucosylated chondroitin sulfate oligomers, we herein report the first detailed mass characterization of fucosylated chondroitin sulfate using high-resolution Fourier transform ion cyclotron resonance mass spectrometry. The two species of fucosylated chondroitin sulfates considered for this work include *Pearsonothuria graeffei* (FCS-Pg) and *Isostichopus badionotus* (FCS-Ib). Fucosylated chondroitin sulfate oligosaccharides were prepared by *N*-deacetylation–deaminative cleavage of the two fucosylated chondroitin sulfates and purified by repeated gel filtration. Accurate mass measurements obtained from electrospray ionization Fourier transform ion cyclotron resonance mass spectrometry measurements confirmed the oligomeric nature of these two fucosylated chondroitin sulfate oligosaccharides with each trisaccharide repeating unit averaging four sulfates per trisaccharide. Collision-induced dissociation of efficiently deprotonated molecular ions through Na/H⁺ exchange proved useful in providing structurally relevant glycosidic and cross-ring product ions, capable of assigning the sulfate modifications on the fucosylated chondroitin sulfate oligomers. Careful examination of the tandem mass spectrometry of both species deferring in the positions of sulfate groups on the fucose residue (FCS-Pg-3,4-OS) and (FCS-Ib-2,4-OS) revealed cross-ring products ^{0,2}A_{αf} and ^{2,4}X_{2αf} which were diagnostic for (FCS-Pg-3,4-OS) and ^{0,2}X_{2αf} diagnostic for (FCS-Ib-2,4-OS). Mass spectrometry and tandem mass spectrometry data acquired for both species varying in oligomer length (dp3–dp15) are presented.

Reprints and permissions: sagepub.co.uk/journalsPermissions.nav

Corresponding author: I Jonathan Amster, Department of Chemistry, University of Georgia, Athens, GA 30602, USA. jamster@uga.edu.

Declaration of conflicting interests

The author(s) declared no potential conflicts of interest with respect to the research, authorship, and/or publication of this article.

Supplementary Material

The Supplementary material for this article is available on the Journal site.

Keywords

FTICR-MS/MS; carbohydrates; fucosylated chondroitin sulfate; sea cucumber

Introduction

Acidic polysaccharides isolated from sea cucumber have been reported to have antithrombic, anti-tumor, and anticoagulant properties and are involved in several biological activities.^{1–9} The two main acidic polysaccharides isolated from sea cucumber include fucosylated chondroitin sulfates (FCSs) and fucan.^{3,10–14} FCS is a rare glycosaminoglycan (GAG) with a backbone similar to that of mammalian chondroitin sulfate, containing large numbers of sulfated α -L-fucopyranosyl (Fuc) branches.^{12,15,16} Their basic trisaccharide repeating unit is composed of [4- β -D-glucuronic acid (GlcA)-1 \rightarrow 3- β -D-N-acetyl galactosamine (GalNAc)-1]_n with the third position of the β -GlcA residue substituted with α -L-Fuc branches.^{17,18} The β -D-GlcNAc unit could be sulfated (S) at the 4-*O*, 6-*O* or both (4, 6-*OS*) whereas the 2-*O* position of its β -D-glucuronic acid unit is unsubstituted.¹⁷ Sulfate modifications on the fucose branches could either be mono-sulfated or di-sulfated depending on the species of sea cucumber from which they are isolated.^{3,6,8,19,20} Recently, the similarity in structure between FCS and GAGs isolated from other tissues has led to investigations about its anticoagulant and antithrombic activities.²¹ Reports of increased anticoagulant activities of FCS have been linked to its ability to increase the inhibition of thrombin and factor Xa by antithrombin or heparin cofactor II.^{2,6,22,23} These observations have been attributed to the sulfated α -L-fucopyranosyl branches.^{3,18,24,25} Notably, desulfation or de-fucosylation of FCS leading to loss of its anticoagulant activities have been reported.^{2,26} Other documented roles of FCS, include their ability to interact with the selectin family of cell-adhesion molecules.⁷ FCS extracted from *Lovenia grisea* shows a 4–8-fold increase in inhibiting interactions of P- and L-selectin with sialyl Lewis^x(sLe^x) antigen compared to heparin. This work further highlighted the fact that the removal of the sulfated fucose branches on FCS obliterated its inhibitory potential in vitro and in vivo. The structure–activity relationship of FCS continues to drive the search for analytical methods that can efficiently elucidate the structural features of these compounds.

Typical of most sulfated polysaccharides, the structural analysis of FCS can be challenging. This is mainly due to variations in sulfation patterns, degree of branching and oligomer length. Nuclear magnetic resonance (NMR)^{3,18,27,28} has been the choice analytical tool for obtaining structural details on FCS; however, limitations due to sample quantity and purity can be problematic.^{29,30} Recently, electrospray ionization (ESI) tandem mass spectrometry analysis of sulfated polysaccharides is emerging as an alternative to NMR as it offers high sensitivity, fast analysis time and requires sub-microgram amounts of sample.²⁹ Electrospray ionization mass spectrometry (ESI-MS) is a widely recognized analytical tool for the analysis of sulfated polysaccharides as they also ionize efficiently in the negative mode.^{31–34} Nevertheless, the labile sulfate groups are susceptible to SO₃ loss during ESI or during ion activation.^{29,35–39} Source and ion transfer optics conditions can be optimized to reduce decomposition of the sulfate groups during ionization and mass analysis.⁴⁰ Labile sulfate groups can be replaced by more stable modifications using a chemical derivatization

procedure, which involves permethylation followed by desulfation and acetylation to improve the analysis of GAGs by online liquid chromatography and tandem mass spectrometry.^{37,38} Additionally, improved tandem mass spectrometry analysis for underivatized dermatan sulfate, heparan sulfate and heparin has been achieved by activating sodium cationized molecular ions to reduce SO₃ loss and improve the amount of product ions observed, especially those occurring from crossring cleavages essential for locating sulfo-modified sites.^{30,35,41,42} Additional information pertaining to the influence of sodium cationized molecular ions on the hexuronic acid stereochemistry of chondroitin, dermatan sulfate and heparan sulfate oligomers has also been reported.^{41–43} Apart from the possibility of sulfation on the fucose ring, the labile nature of the α -L-fucopyranosyl branches can pose a challenge for mass spectrometry (MS) and MS/MS analysis. To date, we have no knowledge of a reported tandem mass spectrometric analysis of FCS. We present for the first time a detailed MS/MS analysis of isolated from *Pearsonothuria graeffei* (FCS-Pg) and *Isostichopus badionotus* (FCS-Ib). These two species differ in the position of the sulfo groups; FCS-Pg is 3,4-*O*-sulfated whereas FCS-Ib is 2,4-*O*-sulfated. Information regarding the location of sulfo groups and differentiation of these two-isomeric species are also discussed.

Methods

Sample preparation and PAGE analysis

Dried sea cucumbers, *P. graeffei* and *I. badionotus*, were locally purchased in Qingdao, China. The FCSs were prepared as previously described.⁴⁴ Briefly, FCS-Pg and FCS-Ib were each extracted from 100 g of dried sea cucumber body wall, digested with protease, precipitated with cetylpyridinium chloride and fractionated using ethanol precipitation.

FCS oligosaccharides were prepared by *N*-deacetylation–deaminative cleavage followed by gel filtration chromatography. The *N*-deacetylation was accomplished by a hydrazinolysis step following the method of Fukuda et al.⁴⁵ Briefly, dried FCS (100 mg) and 1.50 mL hydrazine hydrate containing 1% hydrazine sulfate were added in a reaction tube. The tube was sealed and incubated at 90°C for 12 h on a magnetic stirrer at 250 r/min. After the reaction, the solution was added to 6 mL of ethanol. When several drops of saturated sodium chloride were added, a white precipitate was formed. The precipitate was collected by centrifugation and dissolved in distilled water. This precipitation and dissolution procedure was repeated four times to remove the hydrazine and hydrazine sulfate. The resulting solution was dialyzed against flowing tap water for 2 d and distilled water for 1 d with a 3500 Da molecular weight cutoff and subsequently lyophilized.

Deaminative cleavage followed Bienkowski and Conrad's⁴⁶ method with some modification. Nitrous acid reagent was prepared by mixing 0.5 M H₂SO₄ and 5.5 M NaNO₂ at a volume ratio of 3:5. Deacetylated FCS solution (20 mg in 1 mL ice-cold water) was added to 2 mL of pre-cooled nitrous acid reagent in a reaction tube. The reaction was performed for 10 min in an ice bath, and the excess nitrous acid was neutralized by adding 1.5 mL 0.5 M NaOH. Immediately, 150 μ L of 300 mg/mL NaBH₄ (dissolved in 0.05 M NaOH) was added and allowed to react with the FCS oligosaccharides at 50°C for 2 h. Finally, the sample was dialyzed against distilled water in 500 Da molecular weight cutoff bags and lyophilized.

The resulting oligosaccharide mixtures were fractionated by gel filtration on a Superdex 30 prep grade column (2.6 cm × 120 cm) eluted with 0.3 M NH₄HCO₃ at a flow rate of 0.3 mL/min and were collected in a tube every 6 min. Every tube of sample was analyzed using a Superdex Peptide 10/300 GL column (10 mm × 300 mm) and monitored with a refractive index detector, those showing a single peak of the same retention time were collected together, and five main fractions were collected for each oligosaccharide mixture. Polyacrylamide gel electrophoresis (PAGE) on an isocratic 22% gel stained with Alcian blue⁴⁷ was used to analyze the FCS oligosaccharides that had been fractionated by gel filtration. The size in dp was determined and purity of each FCS oligosaccharide was estimated to be > 80%.

Mass spectrometry analysis

Collision-induced dissociation (CID) experiments were performed on a 9.4 T Bruker Apex Ultra QeFTMS (Billerica, MA). Each sample (0.1 mg/mL) (dp3–dp15) from both species was injected at a rate of 120 µL/h in 50:50 methanol:H₂O and ionized in the negative mode by electrospray using a heated metal capillary (Agilent Technologies, Santa Clara, CA, #G2427A). Dilute amounts of NaOH (1 mM) was added to the spray solvent to stabilize the labile sulfate groups. Multiple charged sodium adducted molecular ions were carefully selected using a 3 Da window and activated using CID. For each spectrum 512 K points were acquired, padded with one zero-fill, and apodized using a sinebell window. External calibration was performed to achieve a mass accuracy of 5 ppm. Internal calibration using confidently assigned glycosidic bond cleavage product ions was also performed to obtain mass accuracy of less than 1 ppm. MS/MS product ions have been assigned using accurate mass measurements and Glycoworkbench.^{48,49} These ions have been illustrated and discussed using both the Domon–Costello⁵⁰ nomenclature and structures obtain from Glycoworkbench.

Results and discussion

ESI accurate mass measurements obtained from intact FCS oligosaccharides confirmed the basic trisaccharide sequence of both FCS species to be [4-β-D-GlcA-1→3-β-D-GalNAc-1]_n with the third position of the β-GlcA acid residues substituted with di-sulfated α-Fuc branches averaging four sulfates per trisaccharide. The modification of the terminal GalNAc to β-3-anhydrotalitol-(4,6-OS) resulting from deaminative cleavage with nitrous acid is also confirmed by high-resolution accurate mass measurements. With the addition of dilute amounts of NaOH to the spray solvent, we are able to observe higher ionized state for the intact FCSs oligomers with their corresponding cationized molecular ions. The annotated ESI-MS for these isomeric FCSs oligomers (dp3–dp15) is included in the online supplementary material (Figures 1–6). The paragraphs below discuss the mass spectrometric results for both species for each degree of polymerization.

MS/MS of FCS-Pg dp3 and FCS-Ib dp3

Negative-mode ESI-MS of both dp3 FCS-Pg and FCS-Ib produced abundant multiply charged molecular ions –4, –3 and –2 as well as their Na⁺ counterions for MS/MS as shown in online supplementary Figure 1. Fully ionized molecular ions considered for the MS/MS

experiment include $[M-5Na-3Na]^{2-}$, $[M-5H-2Na]^{3-}$ and $[M-5H-Na]^{4-}$ with m/z 434.9585, 282.3093 and 205.9846, respectively. Structurally informative fragment ions observed for these molecular ions have enabled the assignment of sulfo modifications especially on the differing fucose units of both isomers FCS-Pg and FCS-Ib. For FCS-Pg, the two sulfo groups 2,3-*OS* located on the fucose residue can be confidently assigned using the accurate masses of cross-ring product ions $^{2,4}X_{2af}$ and $^{0,2}A_{af}$. Confirmatory fragments such as $^{3,5}A_{af}$, $^{3,5}X_{2af}$, $^{0,3}A_{af}$ and $^{0,3}X_{2af}$ can locate the presence of the 4-*O* sulfo group. The symmetric nature of these molecules resulting from the formation of the β -3-anhydrotalitol-(4,6-*OS*) residue which has the same elemental composition as the di-sulfated fucose unit could be challenging especially in the absence of cross-ring product ions. Despite this structural feature of the compound, we can confidently assign the number of sulfates on the fucose ring using the accurate mass of distinct cross-ring products $^{1,5}A_{af}$ and $^{1,4}A_{af}$. Spectra-to-spectra comparison of dp3 FCS-Ib and FCS-Pg reveal cross-ring products $^{0,2}A_{af}$ and $^{2,4}X_{af}$ occurring at m/z 284.9356 and 303.0093 as diagnostic for FCS-Pg (online supplementary Figure 7). Similarly, we observe the highest number of fragmentation for dp3 FCS-Ib on the fucose ring. The accurate mass of the $^{0,3}A_1$ ion occurring from the MS/MS of all the three selected molecular ions can locate the 4-*OS* on the fucose ring. The positions of the two sulfo groups on the fucose ring (2, 4-*OS*) increase the possibility of fragment ions ($^{0,2}A_{af}$ and $^{0,2}X_{2af}$) being isobaric with ($^{2,4}X_0$ and $^{2,4}A_3$) on the β -3-anhydrotalitol residue. However, the $^{0,2}A_n$ and $^{0,2}X_n$ product ions have been reported for MS/MS of 2-*O* and 4-*O* sulfated fucoidan L-fucose isomers⁵¹ of highly sulfated fucan from algal *Laminaria cichorioides*⁵² and *Ascophyllum nodosum*.⁵³ The postulated mechanism supported by computational studies for the occurrence of the $^{0,2}A_n$ and $^{0,2}X_n$ product ions occurring on the L-fucose isomers by Tissot et al. supports a McLafferty rearrangement fragmentation pathway following the cleavage of the C-1–O-5 fucose bond.⁵¹ It is also worth noting from recent EDD^{29,54} and CID^{41,55} reports on mammalian chondroitin, dermatan sulfate and hyaluronic acid⁵⁶ oligosaccharide the rare occurrence of cross-ring fragmentation on the GalNAc residues. The above-referenced works support the $^{0,2}A_{af}$ and $[^{0,2}X_{2af} + 2Na]^{2-}$ ions with m/z 182.9968 and 331.9654, respectively, more likely to occur on the fucose residue. The $[^{0,2}X_{2af} + 2Na]^2$ product ion shown in online supplementary Figure 7 containing three sulfate groups was observed to be diagnostic for FCS-Ib dp3 and can be used to confirm the presence of the 2-*O* sulfo group on FCS-Ib. The position of the 4-*O* sulfo group on the fucose ring is assigned using the accurate mass of the $^{3,5}A_{af}$ ion, with the mass $^{1,5}A_{af}$ confirming the presence of two sulfate groups on the fucose ring. The cross-ring product ions $^{0,2}A_n$, $^{0,2}X_n$, $^{0,3}X_n$ and $^{0,3}A_n$ observed on the fucose residues of both dp3 isomers have also been reported on 2-*O*, 3-*O* and 4-*O* sulfated fucose residues of fucoidan oligosaccharides.^{51–53} The annotated MS/MS spectra comparison for the $[M-5H-Na]^{4-}$ molecular ion for the two isomers is shown in Figure 1. Figure 2 also shows the CID MS/MS structural annotations for all the fully deprotonated molecular ions for dp3 FCS-Pg and FCS-Ib. Only structurally informative product ions are shown in the annotated structures.

MS/MS of FCS-Pg dp6 and FCS-Ib dp6

The structural composition of the dp6 FCS oligomers indicates 10 ionizable protons comprising eight sulfate groups and two carboxyl groups. With the aid of the ESI-MS shown

in online supplementary Figure 2, we are able to confirm the elemental composition of both FCS-Ib and FCS-Pg hexasaccharides. Charged states observed for both isomers ranged from -6 to -3 . The favorable intensities of the fully deprotonated ion $[M-10H + 5Na]^{5-}$ for both FCS-Ib and FCS-Pg dp6 have been considered for MS/MS analysis. Additionally, the abundance of the $[M-9H + 3Na]^{6-}$ observed in the MS of FCS-Pg dp6 proved to be more structurally informative. Figure 3 shows the MS/MS spectra annotations for the $[M-9H + 3Na]^{6-}$ precursor ion for FCS-Pg dp6. Structural annotations showing extensive fragmentation on the fucose ring allowing for the location of the 3, 4-*O* sulfo groups is shown for the $[M-10H + 5Na]^{5-}$ and $[M-9H + 3Na]^{6-}$ molecular ions in Figure 4. The $^{0,2}A_{af}$ ion locates unambiguously the position of both sulfo groups with $^{3,5}A_{af}$, and $^{0,3}A_{af}$ confirming the presence of the 4-*O* sulfo group on the fucose. Complete glycosidic bond fragmentations are also observed including loss of a single and both fucose rings. Figure 5 also shows the structural annotations and MS/MS of FCS-Ib dp6 for the $[M-10H + 5Na]^{5-}$ precursor ion. The cross-ring product ions observed on the fucose ring are very similar to those of dp3 FCS-Ib. We have assigned the two sulfate groups on fucose rings using similar cross-rings ions as discussed for the Ib dp3. As expected, we observe glycosidic cleavages resulting in the loss of fucose residues in both dp6 isomers. Loss of the fucose residue and subsequent loss of sulfate from the fucose residue were observed to dominate the MS/MS spectrum for both isomers. This was expected due to the labile nature of the α -L-Fuc branches and the sulfate half-ester bonds. Again, most cross-ring fragmentations are observed on the Fuc ring residues. Similar to MS/MS of mammalian chondroitin sulfate,^{29,41,54} we observe extensive cross-ring fragmentation on the GlcA units. Fragment ions resulting from internal cleavages are also observed, yielding mostly GalNAc monosaccharide residues in MS/MS spectra of both Pg dp6 and Ib dp6. Internal cleavages resulting from the cleavage of multiple glycosidic bonds have been reported in MS/MS of both branched and linear oligosaccharides.⁵⁷⁻⁶² We are able to confirm the presence of the di-sulfated monosaccharide GalNAc residues from the observed internal cleavages as shown in Figures 3 and 5. Isobaric ions have been designated the same color on the annotated structures of the dp6 isomers as shown in Figures 4 and 5.

MS/MS of FCS-Pg dp9 and FCS-Ib dp9

The MS and MS/MS results for the nonasaccharide isomers for Pg and Ib are discussed below. Precursor ion selection for these isomers was based on the number of ionizable protons deprotonated and ion abundance. For FCS-Pg dp9, the molecular ion $[M-15H + 8Na]^{7-}$ with m/z 380.6834 was subjected to CID activation. This ionized state represents a deprotonation of all the 15 ionizable protons comprising 12 sulfate groups and 3 carboxyl groups. We again observe extensive cross-ring fragmentation on the fucose residues as shown in Figure 6(a). Cross-ring product ions such as $^{3,5}A_{af}$ positions a sulfate group at the 4-*O* position whereas $^{1,4}A_{af}$ ion establishes a di-sulfated fucose ring. Other cross-ring product observed was accompanied with SO_3 losses. It is worth noting that we observed glycosidic product ions adjacent each sugar residue. The structural annotation for CID MS/MS activation of $[M-15H + 7Na]^{8-}$ molecular ion for FCS Ib dp9 is also shown in Figure 6(b). This ionized state represents a complete deprotonation of all the 15 acidic acid groups. The MS/MS result provided sufficient product ions for the assignment of the structure.

MS/MS of FCS-Pg dp12 and FCS-Ib dp12

The elemental composition of both dp12 FCS fractions has been confirmed by accurate mass measurement from ESI-MS. Online supplementary Figure 4 shows the annotated MS spectra for the ions considered for CID analysis. The accompanying sodium cationized molecular ions for example $[M-20H + 10Na]^{10-}$ ensures all the ionizable protons have been deprotonated. For FCS-Pg dp12, the $[M-19H + 10Na]^{9-}$ molecular ion with m/z 392.1942 was selected and subjected to CID activation. Online supplementary Figure 8 shows the CID MS/MS product ion annotations while the structural annotations for FCS-Pg dp12 are shown in Figure 7(a). The MS/MS was mostly dominated by glycosidic bond fragments. A similar fragmentation was observed for the CID activation of the $[M-20H + 10Na]^{10-}$ for FCS-Ib dp12. The selected molecular ion has 19 out of the 20 ionizable protons deprotonated. The annotated MS/MS structure for the observed product ions for FCS-Ib dp12 is shown in Figure 7(b) for the $[M-20H + 10Na]^{10-}$ molecular ion with m/z 355.0722. The accompanying online supplementary material contains the annotated CID spectra showing a selected number of structurally informative ions (online supplementary Figure 9). With all the acidic groups deprotonated, CID activation of the molecular ion yielded abundant cross-ring and glycosidic product ions for the structural assignment. For example, the $^{1,4}A_{cf}$ peak confirms the presence of the two sulfate groups on the fucose residue with the $^{2,5}A_{cf}$ eliminating the presence of a 3-*O* on the FCS-Ib dp12 oligomer.

MS/MS of FCS-Pg dp15 and FCS-Ib dp15

The polymeric structure for both FCS-Ib and FCS-Pg dp15 oligomers have been confirmed from ESI-MS accurate mass measurements. With optimized ionization conditions, we are able to observe higher ionized states for the dp15 oligomers having 25 ionized groups. The MS of FCS-Pg dp15 showing a charged state distribution from -8 to -5 is shown in online supplementary Figure 5. The highest deprotonated molecular ion observed for this oligomer was $[M-23H + 15Na]^{8-}$. However, the $[M-22H + 14Na]^{8-}$ ion with 22 out of the 25 ionizable protons deprotonated was selected for the CID experiment due to its abundance. The insert shown in online supplementary Figure 5 displays the isotopic distribution of the $[M-22H + 14Na]^{8-}$ m/z 560.7070 molecular ion. The annotated MS/MS spectrum for the FCS-Pg dp15 is shown in online supplemental Figure 10. With 22 out of the 25 ionizable protons deprotonated, we observe SO_3 loss fragments from the molecular ion upon CID activation. Figure 8(a) shows the annotated product ion structure for the FCS Pg dp15 oligomer. We show in online supplementary Figure 6, the nine charged state molecular ions $[M-23H + 14Na]^{9-}$ $[M-24 + 15Na]^{9-}$ and $[M-25H + 16Na]^{9-}$ for the ESI-MS of FCS-Ib dp15. The CID MS/MS spectra and structural annotations for FCS-Ib dp15 for the $[M-24 + 15Na]^{9-}$ m/z 500.7373 are shown in online supplementary Figures 11 and 8(b). Compared to the CID spectra for the FCS-Pg dp15, we observe more structurally informative cross-ring product ions on the fucose ring for FCS-Ib dp15. It is worth noting that the MS/MS spectra for both isomers produced abundant glycosidic product ions essential for assigning the number of sulfate per monosaccharide residue. Compared to FCS-Pg dp15, the MS/MS of FCS-Ib dp15 (online supplementary Figure 11) produced very little sulfate loss fragments mainly due to the effective deprotonation of all the acidic groups except for one (24 out of the 25 ionizable protons).

Conclusions

ESI-MS/MS experiments have been carried out on two isomeric FCS samples isolated from two sea cucumber species, *I. badionotus* (FCS-Ib) and *P. graeffei* (FCS-Pg) ranging from dp3–dp15 using a 9.4 T Fourier transform ion cyclotron resonance (FTICR). With the aid of dilute NaOH added to the spray solvents, we are able to achieve efficient deprotonation of the molecular ions of intact FCS oligomers. Our ESI-MS results confirm the polymeric trisaccharide sequence for the FCS samples examined: [4- β -D-GlcA-1 \rightarrow 3- β -D-GalNAc4, (4,6-OS)-1]_n with the third position of the β -glucuronic acid residue substituted with di-sulfated (FCS-Pg (3, 4-OS) from FCS-Ib (2, 4-OS)) α -L-fucopyranosyl branches. With careful selection of efficiently deprotonated molecular ions, we have been able to produce structurally informative MS/MS spectra rich in both glycosidic and cross-ring product ions for assigning sites of sulfation. From accurate mass measurements and spectra comparison of both isomers, we have been able to differentiate both isomers using cross-ring product ions ^{2,4}X_{2af} and ^{0,2}A_{af} observed to be diagnostic for FCS-Pg (3, 4-OS) and ^{0,2}X_{2af} diagnostic for FCS-Ib (2, 4-OS). Future work will focus on extending this method for sequencing other species of FCSs.

Supplementary Material

Refer to Web version on PubMed Central for supplementary material.

Acknowledgments

Funding

The author(s) disclosed receipt of the following financial support for the research, authorship, and/or publication of this article: IA and IJA gratefully acknowledge generous financial support from the National Institutes of Health, grant P41GM103390. This work was also supported by National Science Foundation of China (31301417) and by grants from the China Scholarship Council.

References

1. Fonseca RJ, Mourão PA. Fucosylated chondroitin sulfate as a new oral antithrombotic agent. *Thromb Haemost.* 2006; 96:822–829. [PubMed: 17139379]
2. Mourão PA, Pereira MS, Pavão MS, et al. Structure and anticoagulant activity of a fucosylated chondroitin sulfate from echinoderm sulfated fucose branches on the polysaccharide account for its high anticoagulant action. *J Biol Chem.* 1996; 271:23973–23984. [PubMed: 8798631]
3. Chen S, Xue C, Tang Q, et al. Comparison of structures and anticoagulant activities of fucosylated chondroitin sulfates from different sea cucumbers. *Carbohydr Polym.* 2011; 83:688–696.
4. Mourão PA, Boisson-Vidal C, Tapon-Bretaudière J, et al. Inactivation of thrombin by a fucosylated chondroitin sulfate from echinoderm. *Thromb Res.* 2001; 102:167–176. [PubMed: 11323028]
5. Pomin VH. Marine medicinal glycomics. *Front Cell Infect Microbiol.* 2014; 4:5. [PubMed: 24524028]
6. Wu M, Huang R, Wen D, et al. Structure and effect of sulfated fucose branches on anticoagulant activity of the fucosylated chondroitin sulfate from sea cucumber *Thelecanthina ananas*. *Carbohydr Polym.* 2012; 87:862–868.
7. Borsig L, Wang L, Cavalcante MC, et al. Selectin blocking activity of a fucosylated chondroitin sulfate glycosaminoglycan from sea cucumber effect on tumor metastasis and neutrophil recruitment. *J Biol Chem.* 2007; 282:14984–14991. [PubMed: 17371880]

8. Luo L, Wu M, Xu L, et al. Comparison of physicochemical characteristics and anticoagulant activities of polysaccharides from three sea cucumbers. *Mar Drugs*. 2013; 11:399–417. [PubMed: 23385300]
9. Pereira MS, Mulloy B, Mourão PA. Structure and anticoagulant activity of sulfated fucans: comparison between the regular, repetitive, and linear fucans from echinoderms with the more heterogeneous and branched polymers from brown algae. *J Biol Chem*. 1999; 274:7656–7667. [PubMed: 10075653]
10. Kariya Y, Watabe S, Hashimoto K, et al. Occurrence of chondroitin sulfate E in glycosaminoglycan isolated from the body wall of sea cucumber *Stichopus japonicus*. *J Biol Chem*. 1990; 265:5081–5085. [PubMed: 2108166]
11. Kariya Y, Mulloy B, Imai K, et al. Isolation and partial characterization of fucan sulfates from the body wall of sea cucumber *Stichopus japonicus* and their ability to inhibit osteoclastogenesis. *Carbohydr Res*. 2004; 339:1339–1346. [PubMed: 15113672]
12. Vieira RP, Mourao PA. Occurrence of a unique fucose-branched chondroitin sulfate in the body wall of a sea cucumber. *J Biol Chem*. 1988; 263:18176–18183. [PubMed: 3142869]
13. Nagase H, Enjyoji K-I, Minamiguchi K, et al. Depolymerized holothurian glycosaminoglycan with novel anticoagulant actions: antithrombin III- and heparin cofactor II-independent inhibition of factor X activation by factor IXa-factor VIIIa complex and heparin cofactor II-dependent inhibition of thrombin. *Blood*. 1995; 85:1527–1534. [PubMed: 7888673]
14. Hu Y, Li S, Li J, et al. Identification of a highly sulfated fucoidan from sea cucumber *Pearsonothuria graeffei* with well-repeated tetrasaccharides units. *Carbohydr Polym*. 2015; 134:808–816. [PubMed: 26428188]
15. Myron P, Siddiquee S, Al Azad S. Fucosylated chondroitin sulfate diversity in sea cucumbers: a review. *Carbohydr Polym*. 2014; 112:173–178. [PubMed: 25129732]
16. Mourão PA, Pereira MS. Searching for alternatives to heparin: sulfated fucans from marine invertebrates. *Trends Cardiovasc Med*. 1999; 9:225–232. [PubMed: 11094330]
17. Panagos CG, Thomson DS, Moss C, et al. Fucosylated chondroitin sulfates from the body wall of the sea cucumber *Holothuria forskali*: conformation, selectin binding, and biological activity. *J Biol Chem*. 2014; 289:28284–28298. [PubMed: 25147180]
18. Ustyuzhanina NE, Bilan MI, Dmitrenok AS, et al. The structure of a fucosylated chondroitin sulfate from the sea cucumber *Cucumaria frondosa*. *Carbohydr Polym*. 2017; 165:7–12. [PubMed: 28363577]
19. Yoshida K-I, Minami Y, Nemoto H, et al. Structure of DHG, a depolymerized glycosaminoglycan from sea cucumber, *Stichopus japonicus*. *Tetrahedron Lett*. 1992; 33:4959–4962.
20. Ustyuzhanina NE, Bilan MI, Dmitrenok AS, et al. Structure and biological activity of a fucosylated chondroitin sulfate from the sea cucumber *Cucumaria japonica*. *Glycobiology*. 2016; 26:449–459. [PubMed: 26681734]
21. Mourão PA. Perspective on the use of sulfated polysaccharides from marine organisms as a source of new antithrombotic drugs. *Mar Drugs*. 2015; 13:2770–2784. [PubMed: 25955754]
22. Glauser BF, Pereira MS, Monteiro RQ, et al. Serpin-independent anticoagulant activity of a fucosylated chondroitin sulfate. *Thromb Haemost*. 2008; 100:420–428. [PubMed: 18766257]
23. Pacheco R, Vicente C, Zancan P, et al. Different antithrombotic mechanisms among glycosaminoglycans revealed with a new fucosylated chondroitin sulfate from an echinoderm. *Blood Coagul Fibrinolysis*. 2000; 11:563–573. [PubMed: 10997797]
24. Chen S, Li G, Wu N, et al. Sulfation pattern of the fucose branch is important for the anticoagulant and antithrombotic activities of fucosylated chondroitin sulfates. *Biochim Biophys Acta*. 2013; 1830:3054–3066. [PubMed: 23313164]
25. Fonseca R, Sucupira I, Oliveira S, et al. Improved anticoagulant effect of fucosylated chondroitin sulfate orally administered as gastro-resistant tablets. *Thromb Haemost*. 2017; 117:662–670. [PubMed: 28102426]
26. Mulloy B, Mourao P, Gray E. Structure/function studies of anticoagulant sulphated polysaccharides using NMR. *J Biotechnol*. 2000; 77:123–135. [PubMed: 10674219]
27. Ustyuzhanina NE, Bilan MI, Dmitrenok AS, et al. Two fucosylated chondroitin sulfates from the sea cucumber *Eupentacta fraudatrix*. *Carbohydr Polym*. 2017; 164:8–12. [PubMed: 28325347]

28. Ustyuzhanina NE, Dmitrenok AS, Bilan MI, et al. Variations of pH as an additional tool in the analysis of crowded NMR spectra of fucosylated chondroitin sulfates. *Carbohydr Res.* 2016; 423:82–85. [PubMed: 26895544]
29. Wolff JJ, Laremore TN, Busch AM, et al. Influence of charge state and sodium cationization on the electron detachment dissociation and infrared multiphoton dissociation of glycosaminoglycan oligosaccharides. *J Am Soc Mass Spectrom.* 2008; 19:790–798. [PubMed: 18499037]
30. Wolff JJ, Laremore TN, Busch AM, et al. Electron detachment dissociation of dermatan sulfate oligosaccharides. *J Am Soc Mass Spectrom.* 2008; 19:294–304. [PubMed: 18055211]
31. Zaia J. Mass spectrometry and glycomics. *OMICS.* 2010; 14:401–418. [PubMed: 20443730]
32. Kailemia MJ, Ruhaak LR, Lebrilla CB, et al. Oligosaccharide analysis by mass spectrometry: a review of recent developments. *Anal Chem.* 2013; 86:196–212. [PubMed: 24313268]
33. Zaia J. Glycosaminoglycan glycomics using mass spectrometry. *Mol Cell Proteomics.* 2013; 12:885–892. [PubMed: 23325770]
34. Zaia J. Mass spectrometry of oligosaccharides. *Mass Spectrom Rev.* 2004; 23:161–227. [PubMed: 14966796]
35. Kailemia MJ, Li L, Ly M, et al. Complete mass spectral characterization of a synthetic ultralow-molecular-weight heparin using collision-induced dissociation. *Anal Chem.* 2012; 84:5475–5478. [PubMed: 22715938]
36. Kailemia MJ, Li L, Xu Y, et al. Structurally informative tandem mass spectrometry of highly sulfated natural and chemoenzymatically synthesized heparin and heparan sulfate glycosaminoglycans. *Mole Cell Proteomics.* 2013; 12:979.
37. Huang R, Liu J, Sharp JS. An approach for separation and complete structural sequencing of heparin/heparan sulfate-like oligosaccharides. *Anal Chem.* 2013; 85:5787–5795. [PubMed: 23659663]
38. Huang R, Pomin VH, Sharp JS. LC-MSn analysis of isomeric chondroitin sulfate oligosaccharides using a chemical derivatization strategy. *J Am Soc Mass Spectrom.* 2011; 22:1577. [PubMed: 21953261]
39. Zaia J, Costello CE. Tandem mass spectrometry of sulfated heparin-like glycosaminoglycan oligosaccharides. *Anal Chem.* 2003; 75:2445–2455. [PubMed: 12918989]
40. Huang Y, Yu X, Mao Y, et al. De novo sequencing of heparan sulfate oligosaccharides by electron-activated dissociation. *Anal Chem.* 2013; 85:11979–11986. [PubMed: 24224699]
41. Kailemia MJ, Patel AB, Johnson DT, et al. Differentiating chondroitin sulfate glycosaminoglycans using collision-induced dissociation; uronic acid crossring diagnostic fragments in a single stage of tandem mass spectrometry. *Eur J Mass Spectrom.* 2015; 21:275–285.
42. Agyekum I, Patel AB, Zong CL, et al. Assignment of hexuronic acid stereochemistry in synthetic heparan sulfate tetrasaccharides with 2-O-sulfo uronic acids using electron detachment dissociation. *Int J Mass Spectrom.* 2015; 390:163–169. [PubMed: 26612977]
43. Agyekum I, Zong C, Boons G-J, et al. Single stage tandem mass spectrometry assignment of the C-5 uronic acid stereochemistry in heparan sulfate tetrasaccharides using electron detachment dissociation. *J Am Soc Mass Spectrom.* 2017; 43:1–10.
44. Li S, Li J, Zhi Z, et al. Macromolecular properties and hypolipidemic effects of four sulfated polysaccharides from sea cucumbers. *Carbohydr Polym.* 2017; 173:330–337. [PubMed: 28732873]
45. Fukuda M, Kondo T, Osawa T. Studies on hydrazinolysis of glycoproteins – core structures of oligosaccharides obtained from porcine thyroglobulin and pineapple stem bromelain. *J Biochem.* 1976; 80:1223–1232. [PubMed: 1035216]
46. Bienkowski MJ, Conrad HE. Structural characterization of the oligosaccharides formed by depolymerization of heparin with nitrous-acid. *J Biol Chem.* 1985; 260:356–365. [PubMed: 3965453]
47. Rice KG, Rottink MK, Linhardt RJ. Fractionation of heparin-derived oligosaccharides by gradient polyacrylamide-gel electrophoresis. *Biochem J.* 1987; 244:515–522. [PubMed: 3446173]
48. Ceroni A, Maass K, Geyer H, et al. GlycoWorkbench: a tool for the computer-assisted annotation of mass spectra of glycans. *J Proteome Res.* 2008; 7:1650–1659. [PubMed: 18311910]

49. Damerell, D., Ceroni, A., Maass, K., et al. Annotation of glycomics MS and MS/MS spectra using the GlycoWorkbench software tool. In: Lutteke, T., Frank, M., editors. Glycoinformatics. New York: Springer Science + Business Media; 2015. p. 3-15.
50. Domon B, Costello CE. A systematic nomenclature for carbohydrate fragmentations in FAB-MS/MS spectra of glycoconjugates. *Glycoconjugate J.* 1988; 5:397–409.
51. Tissot B, Salpin J-Y, Martinez M, et al. Differentiation of the fucoidan sulfated L-fucose isomers constituents by CE-ESIMS and molecular modeling. *Carbohydr Res.* 2006; 341:598–609. [PubMed: 16413001]
52. Anastuyk SD, Shevchenko NM, Nazarenko EL, et al. Structural analysis of a highly sulfated fucan from the brown alga *Laminaria cichorioides* by tandem MALDI and ESI mass spectrometry. *Carbohydr Res.* 2010; 345:2206–2212. [PubMed: 20813351]
53. Daniel R, Chevolut L, Carrascal M, et al. Electrospray ionization mass spectrometry of oligosaccharides derived from fucoidan of *Ascophyllum nodosum*. *Carbohydr Res.* 2007; 342:826–834. [PubMed: 17280652]
54. Leach FE, Ly M, Laremore TN, et al. Hexuronic acid stereochemistry determination in chondroitin sulfate glycosaminoglycan oligosaccharides by electron detachment dissociation. *J Am Soc Mass Spectrom.* 2012; 23:1488–1497. [PubMed: 22825742]
55. Zaia J, Li X-Q, Chan S-Y, et al. Tandem mass spectrometric strategies for determination of sulfation positions and uronic acid epimerization in chondroitin sulfate oligosaccharides. *J Am Soc Mass Spectrom.* 2003; 14:1270–1281. [PubMed: 14597117]
56. Tao L, Song F, Xu N, et al. New insights into the action of bacterial chondroitinase AC I and hyaluronidase on hyaluronic acid. *Carbohydr Polym.* 2017; 158:85–92. [PubMed: 28024546]
57. Shi SD-H, Hendrickson CL, Marshall AG, et al. Structural validation of saccharomicins by high resolution and high mass accuracy Fourier transform-ion cyclotron resonance-mass spectrometry and infrared multiphoton dissociation tandem mass spectrometry. *J Am Soc Mass Spectrom.* 1999; 10:1285–1290.
58. Brüll L, Heerma W, Thomas-Oates J, et al. Loss of internal 1→ 6 substituted monosaccharide residues from underivatized and per-O-methylated trisaccharides. *J Am Soc Mass Spectrom.* 1997; 8:43–49.
59. Ková ik V, Hirsch J, Ková P, et al. Oligosaccharide characterization using collision-induced dissociation fast atom bombardment mass spectrometry: evidence for internal monosaccharide residue loss. *J Mass Spectrom.* 1995; 30:949–958.
60. Stephens E, Maslen SL, Green LG, et al. Fragmentation characteristics of neutral N-linked glycans using a MALDI-TOF/TOF tandem mass spectrometer. *Anal Chem.* 2004; 76:2343–2354. [PubMed: 15080747]
61. Harvey DJ. Fragmentation of negative ions from carbohydrates: part 1. Use of nitrate and other anionic adducts for the production of negative ion electrospray spectra from N-linked carbohydrates. *J Am Soc Mass Spectrom.* 2005; 16:622–630. [PubMed: 15862764]
62. Zhao C, Xie B, Chan SY, et al. Collisionally activated dissociation and electron capture dissociation provide complementary structural information for branched permethylated oligosaccharides. *J Am Soc Mass Spectrom.* 2008; 19:138–150. [PubMed: 18063385]

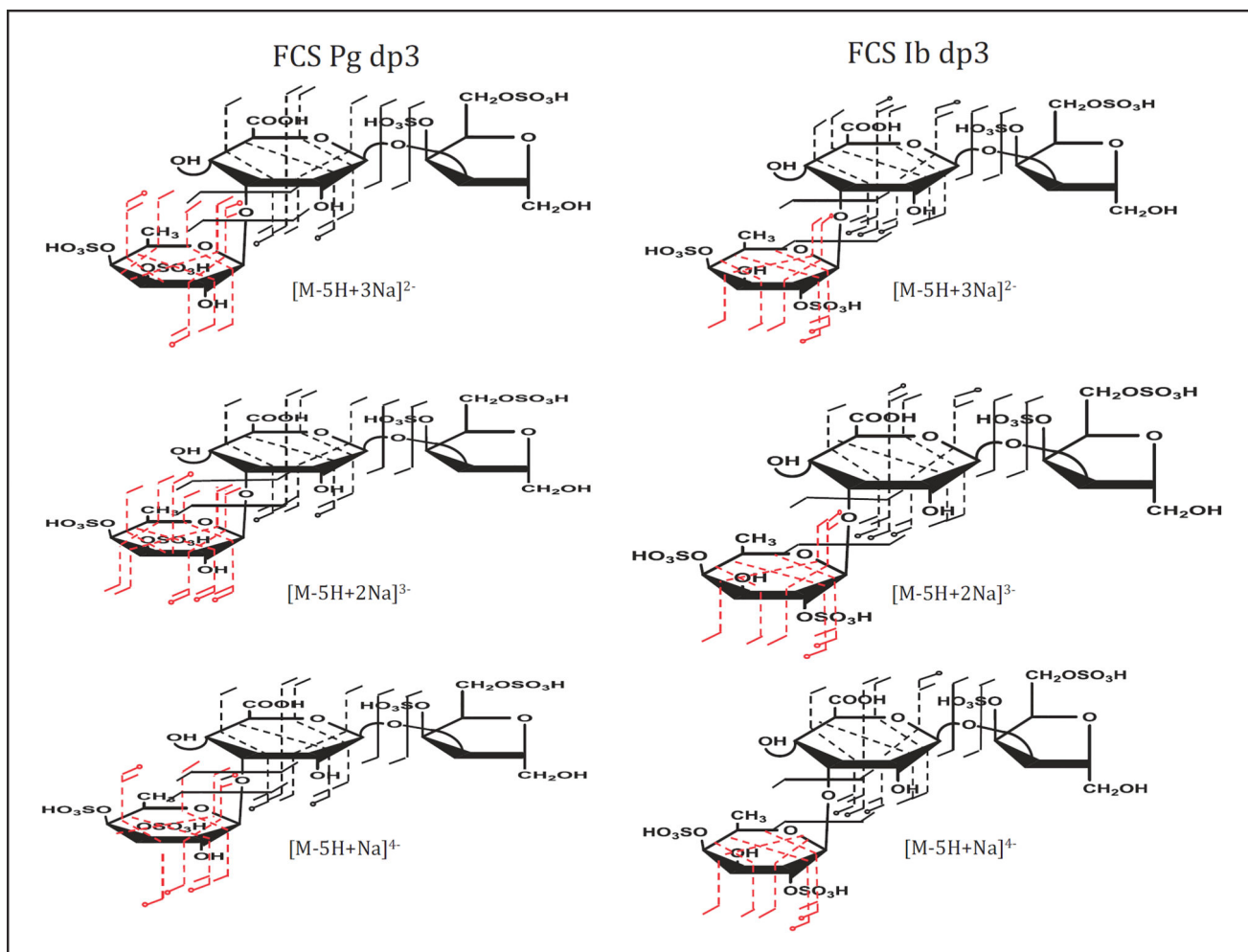


Figure 2.

Structural annotations for CID activation of [M-5H + 3Na]²⁻, [M-5H + 2Na]³⁻ and [M-5H + Na]⁴⁻ molecular ions for FCS Pg dp3 and FCS Ib dp3.

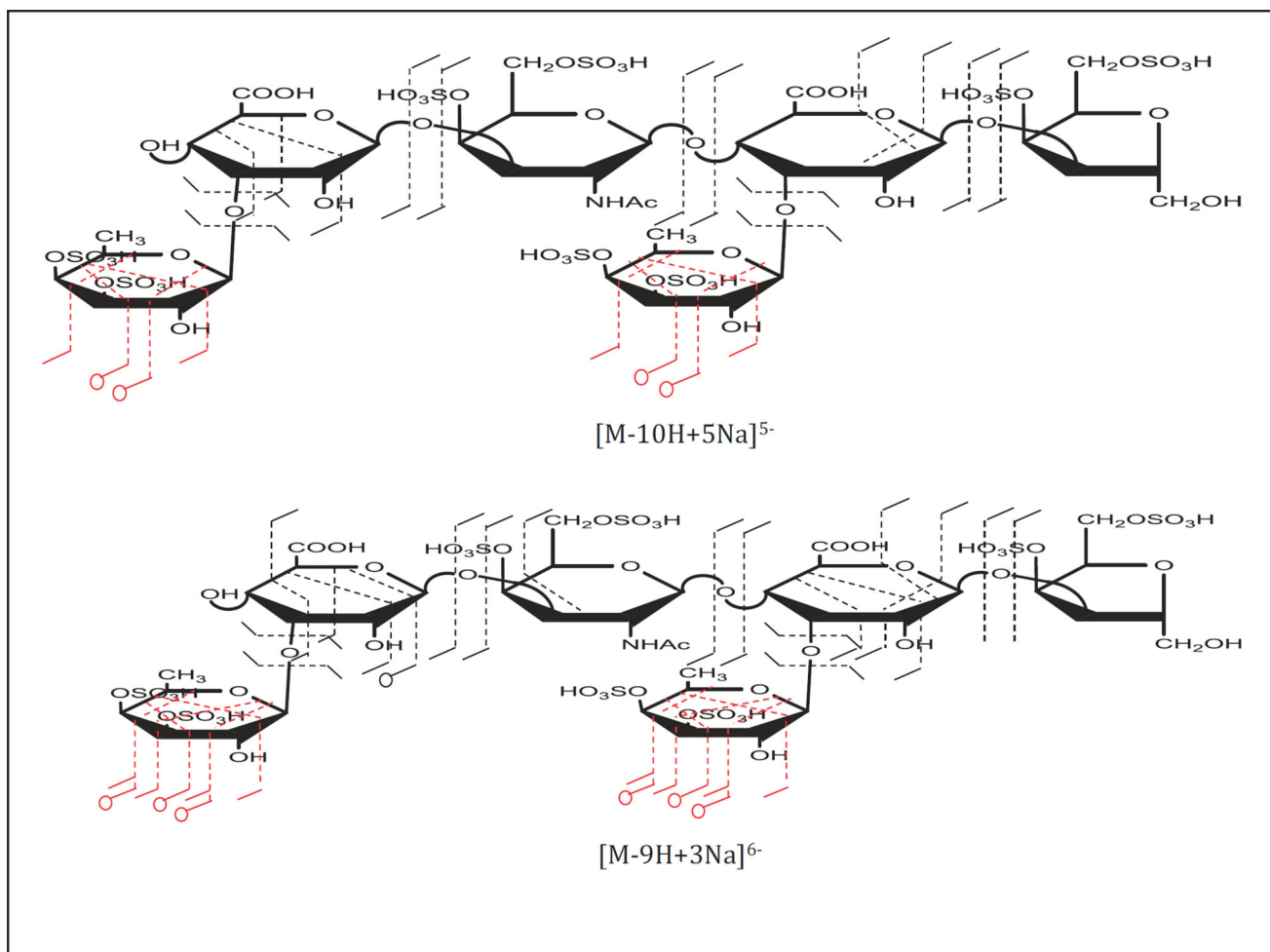


Figure 4. Structural annotations from observed CID fragments for FCS Pg dp6 for the $[M-10H + 5Na]^{5-}$ and $[M-9H + 3Na]^{6-}$ molecular ions.

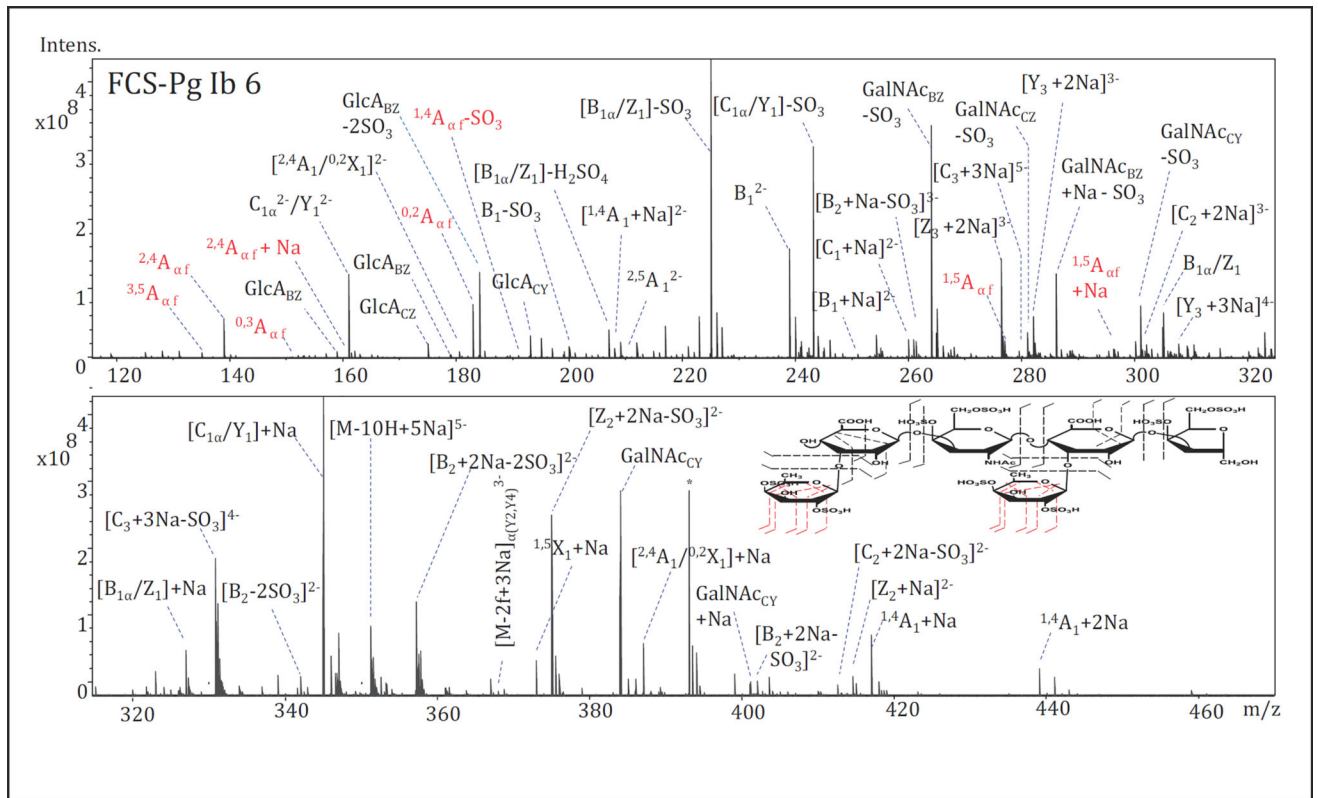
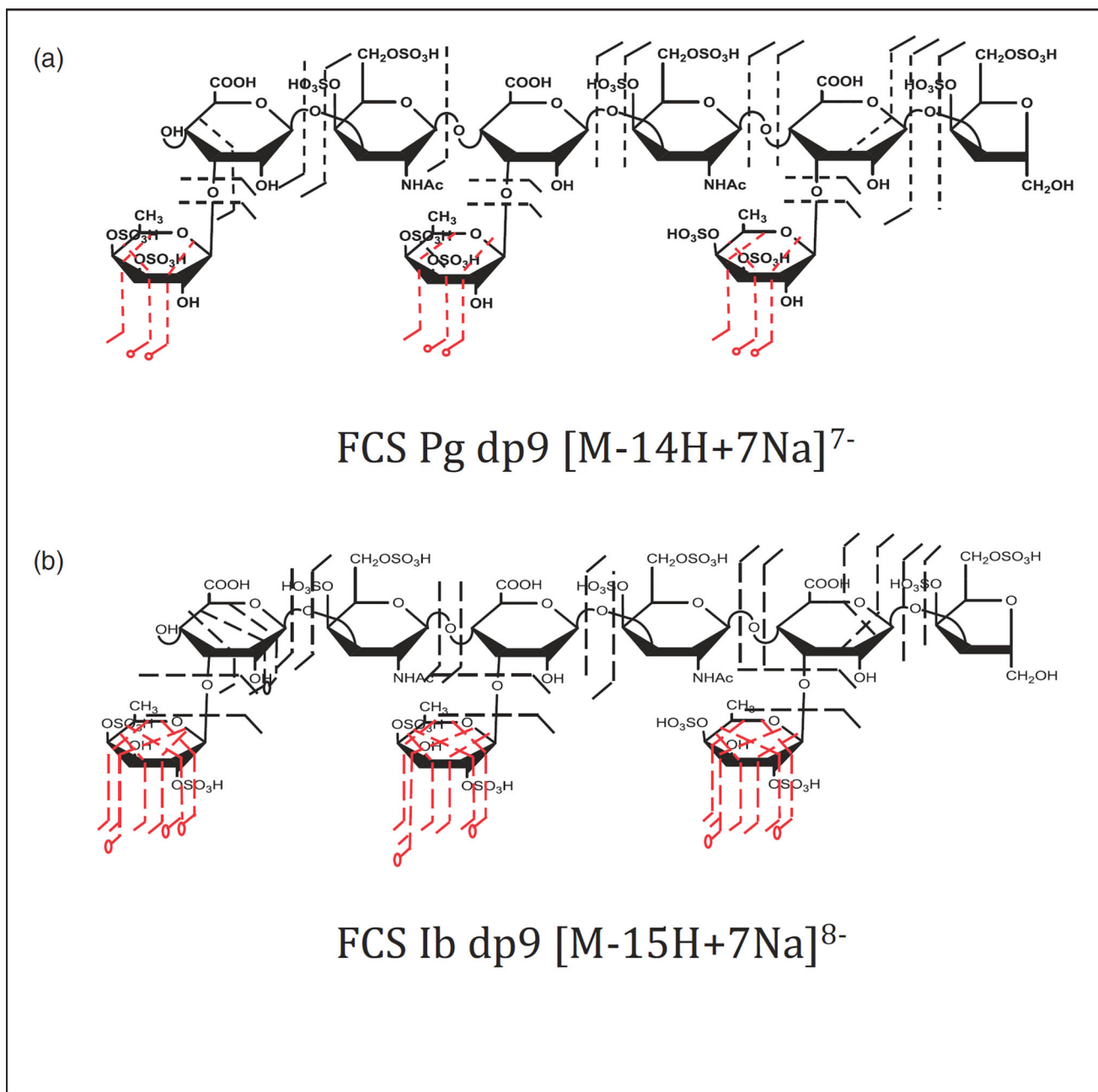
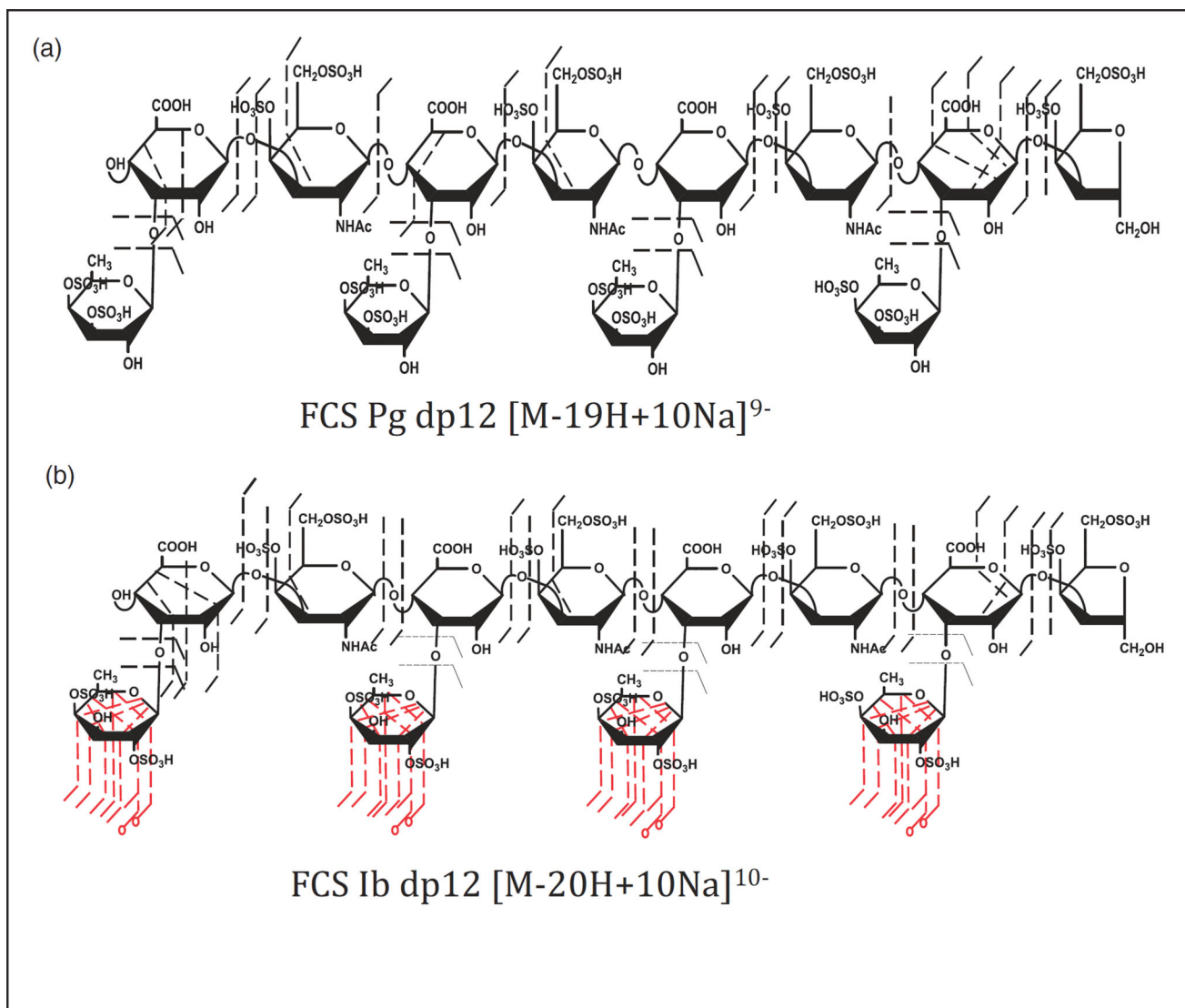


Figure 5. CID MS/MS spectra annotations for the $[M-10H + 5Na]^{5-}$ molecular ion for FCS Ib dp6.

**Figure 6.**

CID structural annotations for (a) [M-14H + 7Na]⁷⁻ molecular ion for FCS Pg dp9 and (b) [M-15H + 7Na]⁸⁻ molecular ion for FCS Ib dp9.

**Figure 7.**

CID MS/MS and structural annotations for (a) the [M-19H + 10Na]⁹⁻ molecular ion for FCS Pg dp12 and (b) the [M-20H + 9Na]¹⁰⁻ molecular ion for FCS Ib dp12.

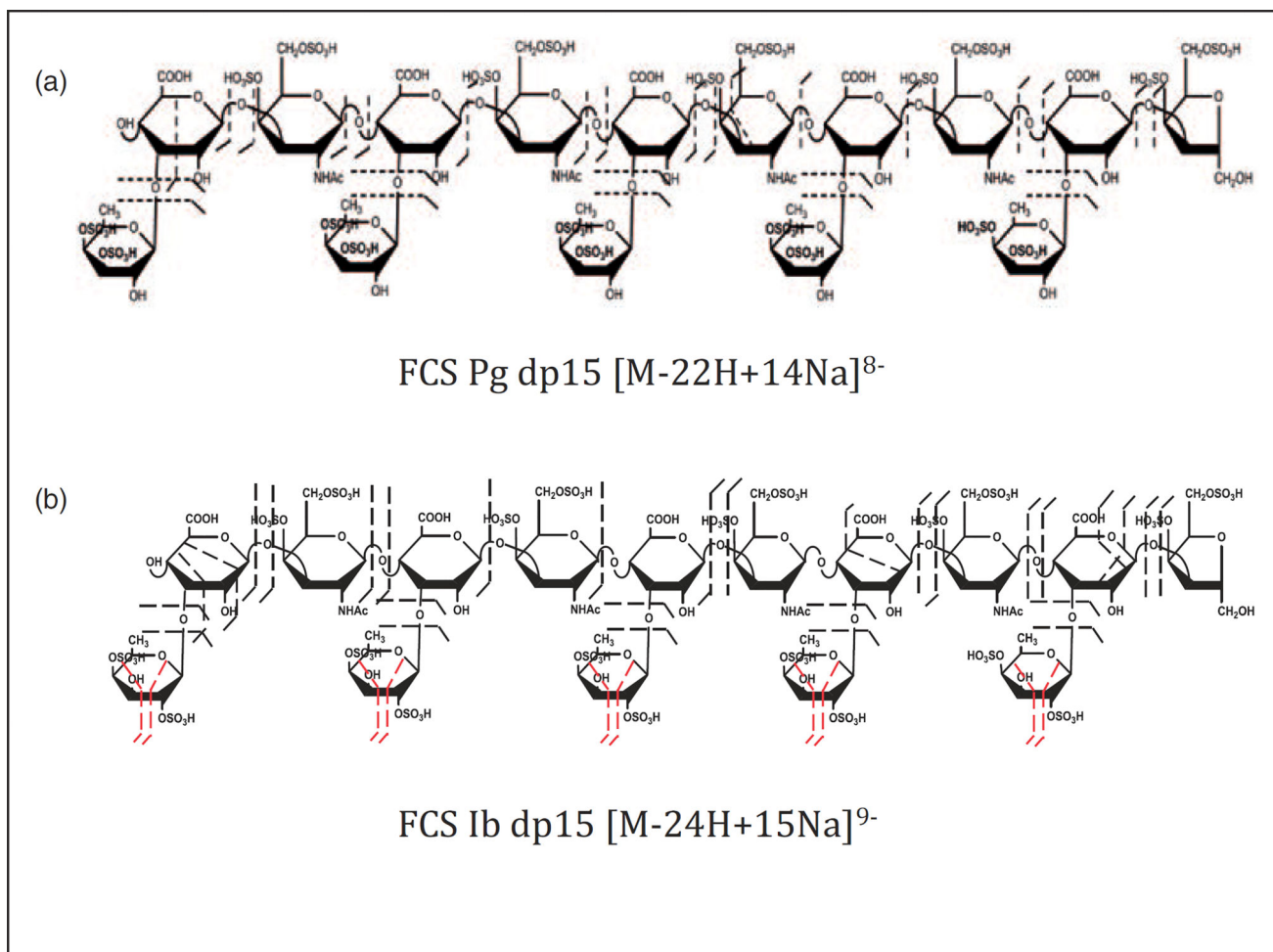


Figure 8. CID MS/MS structural annotations for (a) the [M-22H + 14Na]⁸⁻ molecular ion for FCS Pg dp15 and (b) the structural annotations for the [M-24H + 15Na]⁹⁻ molecular ion for FCS Ib dp15.